IEEE Access
Multidisciplinary | Rapid Review | Open Access Journal

Received October 18, 2018, accepted November 13, 2018, date of publication November 19, 2018,
date of current version December 19, 2018.

Digital Object Identifier 10.1109/ACCESS.2018.2882249

Impact of Mode Decision Delay on Estimation Error in Continuous-Time Controlled System

SHENGWEN XIANG, HONGQI FAN, AND QIANG FU
National Key Laboratory of Science and Technology on ATR, National University of Defense Technology, Changsha 410073, China
Corresponding author: Hongqi Fan (fanhongqi@nudt.edu.cn)

ABSTRACT For highly maneuvering target interception in terminal guidance, the maximal admissible mode decision delay (MAMDD) and the least required mode sojourn time (LRMST) are calculated in continuous-time controlled system. The lateral acceleration command of the evader is modeled as a jump-Markov process. Suppose that the mode switches are observable and the evader's motion mode is correctly identified by a separate mode decision-maker with a fixed time delay, then the error model of the state estimation is derived. By limiting the state estimation error to a certain range, MAMDD and LRMST are calculated. The derivation is validated by a typical instance of tactical ballistic missile interception. The results in this paper provide a useful tool for guiding the design of the mode decision-maker and evaluating the performance of the logic-based integrated estimation and guidance system.

INDEX TERMS Continuous-time controlled system, highly maneuvering target interception, least required mode sojourn time, maximal admissible mode decision delay, state estimation error.

NOMENCLATURE

P	Pursuer/Interceptor
E	Evader/Target
τ_p, τ_e	Time constants of P and E
$a_p^{\max}$, $a_e^{\max}$	Maximum lateral accelerations of P and E
V_p, V_e	Velocities of P and E
u_p, u_e	Lateral acceleration commands of P and E
r	Relative range between players
t_{sw}	Mode switch moment
Δt	Mode decision delay
t_f	Final time
m	Target motion mode
m_{i-1}, m_i	Mode before and after ith mode change
Δm	Mode change value, $\Delta m \triangleq m_i - m_{i-1}$
σ_θ	Angular measurement accuracy
σ_a	Acceleration measurement accuracy
s_w	Power spectral density of process noise
$\tilde{\mathbf{x}}$	State estimation error
ς	Mean error of state estimation
E_0	Error bound
E	Normalized error bound, $E \triangleq E_0/\Delta m_i$
E_∞	Normalized error limit
s_i	Mode sojourn time, $s_i \triangleq t_i - t_{i-1}$

I. INTRODUCTION

With the increasing maneuverability of the evader, highly maneuvering target interception (HMTI) has attracted extensive attention in the research community [1]–[3]. Estimation, guidance and control constitute the three essential factors for a successful interception. Among these, the estimation accuracy of the target state determines the bound of the interception performance. That is, regardless of how the flight system is designed, the error in statistical miss distance will not be lower than the performance guaranteed by the estimator [4].

For HMTI, the state estimation process can be treated as a problem of maneuvering target tracking (MTT). As the maneuvers of the evader are often unknown and unpredictable to the system, a hybrid estimation problem consisting of base state estimation and mode decision is usually needed. The widely used methods for hybrid estimation problems can be basically classified into two categories: the single-model and the multiple-model. Li and Vesselin [5], [6] conducted a series of detailed analyses and comparisons in the context of these techniques. Either way, the mode decision delay affects the estimation performance significantly [7]. Shinar *et al.* [8] figured out that the estimation delay of the target maneuver, especially the delay of the evader's lateral acceleration, is the main error source in miss distance for HMTI. Due to the mode decision delay, mode mismatch occurs once the

evader's mode is switched. It causes a significant deterioration of the estimation performance and may even result in the divergence of the estimator (the mode decision delay is too great and there is insufficient time for the estimator to converge), further affects the guidance performance. Consequently, lowering the impact of mode decision delay is very essential for a precise interception. Related work mainly covers two aspects: exploring new guidance law compensating the estimation delay [9], [10] and reducing the mode decision delay of the target maneuver [11]–[13]. For the latter case, the idea of integrated estimation and guidance (IEG) method, which combines a low-bandwidth highly precise estimator and a separate mode decision-maker that estimates the current motion mode of the evader timely, has been demonstrated superiority for HMTI problems [14]–[16]. The logic-based IEG method proposed by Shinar is one of the most promising algorithms [15]. In fact, both the radar and the image seeker can observe signatures highly related to the target maneuvers, showing some potential to quick mode decision for the mode decision-maker.

To guarantee an ideal guidance performance, the mode decision delay should be limited to a range as small as possible. Therefore, following questions need to be further emphasized. Given the error bound, what is the maximal admissible mode decision delay (MAMDD) for the mode decision-maker to discriminate the evader's motion mode? Once the mode decision delay is settled, what is the least required mode sojourn time (LRMST) to ensure the observability of the mode switches? For these problems, in our previous work, [17] studied the characteristics of state estimation error in discrete-time controlled system and derived the upper bound of mode delay (MDUB) and the lower bound of mode sojourn time (STLB).

In real applications, the sampling interval affects the stability and accuracy of the discrete-time system significantly, thus it is necessary to theoretically analyze the two key parameters for the mode decision-maker in the continuous control system. As a counterpart of [17], the main work and contributions in this paper mainly cover the following two aspects. Firstly, the error model of the state estimation in continuous-time controlled system is derived and validated by Monte Carlo simulations. Secondly, MAMDD is calculated by limiting the state estimation error to a certain range and LRMST is solved once the mode decision delay is given. Compared to [17], a more compact bound is obtained, meaning that a more precise requirement is applied to the mode decision-maker in the stage of designing a practical IEG system. Furthermore, in order to describe the meaning of the two bounds more precisely, MDUB and STLB in [17] are renamed as MAMDD and LRMST in present work, respectively.

The remainder of the paper is organized as follows: Section 2 describes the mathematical model in a planar interception scenario. Section 3 derives the state estimation error model in continuous time. Section 4 calculates MAMDD and LRMST with a given estimation error bound. Demonstrations and conclusions are presented in Section 5 and Section 6, respectively.

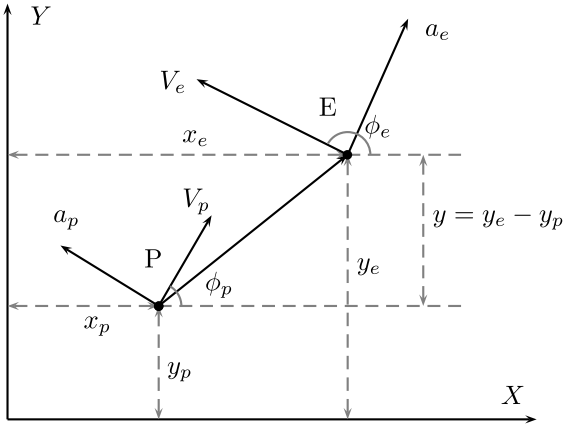

FIGURE 1. Planer interception geometry. The X axis lies along the initial line of sight. (x_p, y_p) and (x_e, y_e) are current positions of P and E, respectively. ϕ_p and ϕ_e are the aspect angles defined as the angles between the velocity vectors and the positive X axis.

II. PROBLEM FORMULATION

A. SYSTEM MODEL

Similar to most work discussed the interception problem, the engagement takes place in a horizontal planar consisting of two players [3], [14]–[18] – a pursuer (interceptor) denoted by P and an evader (target) denoted by E – as shown in Fig. 1. Three basic assumptions for a planer interception are made as follows:

- Both dynamics of the players are approximated by the first-order transfer functions, with the time constants τ_p and τ_e, respectively;
- Both speeds of the players are constant, denoted by V_p and V_e, respectively;
- Both lateral accelerations of the players are bounded, with maximal values $a_p^{\max}$ and $a_e^{\max}$, respectively.

Fig. 1 shows the planer interception geometry. Due to the short duration of the terminal guidance and the high velocities involved in HMTI, the aspect angles here satisfy the small angle conditions (that is, $\sin\phi_p \approx \phi_p$, $\sin\phi_e \approx \pi - \phi_e$). Therefore, the trajectories can be linearized along the initial line of sight. Let the initial time $t_0 = 0$s and given the initial range r_0, the final time t_f of the interception can be easily approximated as

$$t_f \approx \frac{r_0}{V_p \cos\phi_p(0) - V_e \cos\phi_e(0)} \tag{1}$$

Denote the state vector $\mathbf{x} = [x_1(t), x_2(t), x_3(t), x_4(t)]^{\mathrm{T}} = [y(t), \dot{y}(t), a_y^e(t), a_y^p(t)]^{\mathrm{T}}$, where $t \in [0, t_f]$. For brevity, the time t is omitted hereafter. Based on the above assumptions, the system dynamics can be modeled with the following linear differential equations:

$$\begin{aligned} \dot{x}_1 &= x_2, \quad x_1(0) = 0 \\ \dot{x}_2 &= x_3 - x_4, \quad x_2(0) = V_e\phi_e(0) - V_p\phi_p(0) \end{aligned}$$

$$\dot{x}_3 = (u_e - x_3)/\tau_e, \quad x_3(0) = 0$$
$$\dot{x}_4 = (u_p - x_4)/\tau_p, \quad x_4(0) = 0 \tag{2}$$

where $x_1 = y_e - y_p$ is the relative range between P and E along the Y axis; x_2 is the relative lateral velocity; x_3 and x_4 are the lateral accelerations of P and E, respectively; u_p and u_e are the respective commanded accelerations bounded by

$$|u_i(t)| \le a_i^{\max}, \quad i = p, e \tag{3}$$

Eq. (2) can be represented as the following state vector form

$$\dot{\mathbf{x}} = \mathbf{A}\mathbf{x} + \mathbf{B}_1 u_p + \mathbf{B}_2 u_e, \quad \mathbf{x}(0) = (0, x_2(0), 0, 0)^{\mathrm{T}} \tag{4}$$

where matrixes $\mathbf{A}$, $\mathbf{B}_1$ and $\mathbf{B}_2$ are given by

$$\mathbf{A} = \begin{bmatrix} 0 & 1 & 0 & 0 \\ 0 & 0 & 1 & -1 \\ 0 & 0 & -1/\tau_e & 0 \\ 0 & 0 & 0 & -1/\tau_p \end{bmatrix}, \quad \mathbf{B}_1 = \begin{bmatrix} 0 \\ 0 \\ 0 \\ 1/\tau_p \end{bmatrix},$$
$$\mathbf{B}_2 = \begin{bmatrix} 0 \\ 0 \\ 1/\tau_e \\ 0 \end{bmatrix} \tag{5}$$

B. JUMP-MARKOV ACCELERATION COMMAND MODEL

Assume that the lateral acceleration command of the evader follows a Jump-Markov process [11]

$$u_e(t) = m(t) + w(t) \tag{6}$$

where $m(t)$ is the discretized mode of evader's lateral acceleration command shown in Fig. 2, and $w(t)$ is the quantizing error treated as a zero-mean Gaussian white noise with the power spectrum density s_w. For detailed methods of mode-set design with respect to MTT, one can refer to [11], [19], and [20].

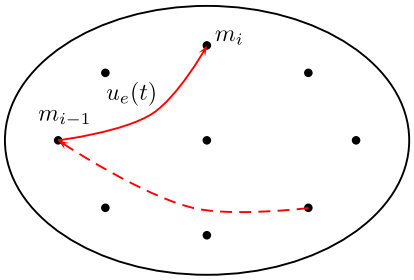

FIGURE 2. Model-set of the evader's lateral acceleration command. The mode space is discretized and the acceleration command of the evader jumps from one mode to another. m_i represents the specific acceleration command at time t_i.

C. OBSERVATION MODEL

To be consistent with [17], we use the following observation model

$$\mathbf{Y}(t) = \mathbf{H}\mathbf{x}(t) + \mathbf{v}(t) \tag{7}$$

where $\mathbf{Y}(t) = [y_m, a_{ym}^p]^{\mathrm{T}}$ is the measurement vector (y_m and a_{ym}^p are the measurements of the relative position and the pursuer's acceleration, respectively), $\mathbf{H}$ is the measurement matrix given by

$$\mathbf{H} = \begin{bmatrix} 1 & 0 & 0 & 0 \\ 0 & 0 & 0 & 1 \end{bmatrix}, \tag{8}$$

and $\mathbf{v}(t)$ is the observation noise obeying the Gaussian distribution with zero mean and covariance $\mathbf{R}(t)$ [17]. The pursuer's acceleration is measured by the onboard accelerometer precisely, thus its measurement noise is of a relatively small variance σ_a^2.

III. STATE ESTIMATION ERROR MODEL

Fig. 3 shows a typical structure of the logic-based IEG system, where the estimator is independently optimized from the controller. For this configuration, a separate mode decision-maker is used to estimate the evader's current motion mode $m(t)$. Each $m(t)$ corresponds to a model, which increases the flexibility to the system for a number of different models. Therefore, a timely and accurate mode decision-maker is beneficial for the estimator to choose the matched mode quickly and correctly. Furthermore, it also helps the guidance processor to choose the proper guidance law and its parameters when a mode change occurs. For example, if the absolute value of $m(t)$ is small enough, DGL/0 (DGL: differential game law) may be preferable because it is more robust and efficient; if the absolute value of $m(t)$ is large, DGL/1 will be more appropriate; if the sign or direction of $m(t)$ is known, it will be further used to reduce the reachable set [21] of target acceleration when calculating ZEM. Based on this configuration, in the following, the error model of the state in continuous-time controlled system is derived.

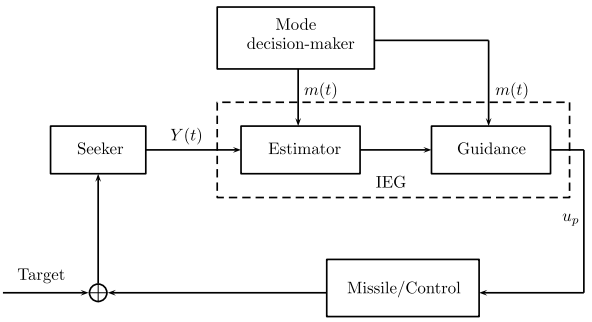

FIGURE 3. A typical structure of IEG system. $\mathbf{Y}(t)$ is the observation vector of the seeker. $m(t)$ is the output of the mode decision-maker. u_p is the control command generated by guidance law.

Assume that the current motion mode of the evader is correctly identified by the mode decision-maker with a fixed time delay Δt after the mode switching moment. Let the mode after the ith mode change be m_i, then the mode switch processes and the corresponding outputs of the mode decision-maker are illustrated in Fig. 4.

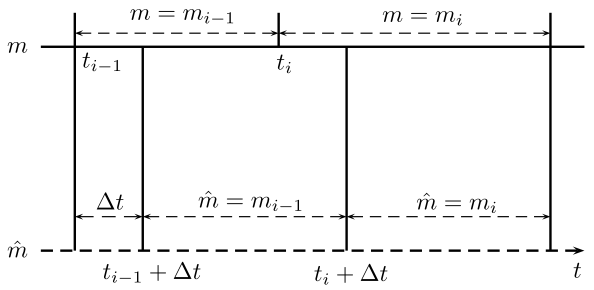

FIGURE 4. Diagram of mode switch and the outputs of the mode decision-maker. m and $\hat{m}$ represent the actual and the estimated acceleration command of the evader, respectively. A certain mode decision delay Δt exits in the process of mode identification.

Consider time $t_{i-1} \leq t \leq t_{i+1}$, then $m(t)$ can be expressed as

$$m(t) = m_{i-1} + (m_i - m_{i-1})u(t - t_i) \tag{9}$$

where $u(t)$ is the step function given by

$$u(t) = \begin{cases} 1, & t \geq 0 \\ 0, & t < 0 \end{cases} \tag{10}$$

From Fig. 4, the dynamic model used by the estimator can be formulated as

$$\dot{\mathbf{x}}(t) = \mathbf{A}\mathbf{x}(t) + \mathbf{B}_1 u_p(t) + \mathbf{B}_2(m_i - m_{i-1})u(t - t_i - \Delta t) + \mathbf{w}(t) \tag{11}$$

Substituting Eq. (6) into Eq. (4) yields

$$\dot{\mathbf{x}}(t) = \mathbf{A}\mathbf{x}(t) + \mathbf{B}_1 u_p(t) + \mathbf{B}_2 m(t) + \mathbf{w}(t) \tag{12}$$

where $\mathbf{w}(t) = \mathbf{B}_2 w(t)$ is the process noise that follows a zero-mean Gaussian distribution with covariance matrix $\mathbf{Q} = \mathbf{B}_2\mathbf{B}_2^{\mathrm{T}} s_w$. Without loss of generality, only the error distribution during the time $t \in [t_{i-1} + \Delta t, t_i + \Delta t]$ is considered here. Two cases need to be taken into account specifically.

Case 1: $t \in [t_{i-1} + \Delta t, t_i)$. The corresponding motion mode of the evader is m_i, then the system state equation is

$$\dot{\mathbf{x}}(t) = \mathbf{A}\mathbf{x}(t) + \mathbf{B}_1 u_p(t) + \mathbf{B}_2 m_{i-1} + \mathbf{w}(t) \tag{13}$$

The standard Kalman filter is used as the estimator, then the form of the observer is governed by

$$\dot{\hat{\mathbf{x}}}(t) = \mathbf{A}\hat{\mathbf{x}}(t) + \mathbf{B}_1 u_p(t) + \mathbf{B}_2 m_{i-1} + \mathbf{k}(t)(\mathbf{Y}(t) - \mathbf{H}\hat{\mathbf{x}}(t)) \tag{14}$$

where $\mathbf{k}(t)$ is the Kalman gain in continuous system given by

$$\mathbf{k}(t) = \mathbf{P}(t)\mathbf{H}^{\mathrm{T}}\mathbf{R}^{-1} \tag{15}$$

$\mathbf{P}(t)$ is the covariance matrix of prediction error specified by the following Riccati equation

$$\dot{\mathbf{P}}(t) = \mathbf{A}\mathbf{P}(t) + \mathbf{P}(t)\mathbf{A}^{\mathrm{T}} + \mathbf{Q} - \mathbf{P}(t)\mathbf{H}^{\mathrm{T}}\mathbf{R}^{-1}\mathbf{H}\mathbf{P}(t) \tag{16}$$

The state estimation error is defined as the difference between the estimated state and the real state. That is, $\tilde{\mathbf{x}}(t) = \hat{\mathbf{x}}(t) - \mathbf{x}(t)$. Subtracting Eq. (13) from Eq. (14) yields

$$\begin{aligned} \dot{\tilde{\mathbf{x}}}(t) &= (\mathbf{A} - \mathbf{k}(t)\mathbf{H})\tilde{\mathbf{x}}(t) + (\mathbf{k}(t)\mathbf{v}(t) - \mathbf{w}(t)) \\ \tilde{\mathbf{x}}(t_{i-1} + \Delta t) &= \tilde{\mathbf{x}}_{t_{i-1}+\Delta t} \end{aligned} \tag{17}$$

Denote $\mathbf{F}(t) = \mathbf{A} - \mathbf{k}(t)\mathbf{H}$ and $\xi(t) = \mathbf{k}(t)\mathbf{v}(t) - \mathbf{w}(t)$, respectively. Solving Eq. (17), we have

$$\begin{aligned} \tilde{\mathbf{x}}(t) = \exp\left\{\int_{t_{i-1}+\Delta t}^{t} \mathbf{F}(s)\mathrm{d}s\right\} \tilde{\mathbf{x}}_{t_{i-1}+\Delta t} \\ + \int_{t_{i-1}+\Delta t}^{t} \exp\left\{\int_{s}^{t} \mathbf{F}(u)\mathrm{d}u\right\} \xi(\mathrm{s})\mathrm{d}s \end{aligned} \tag{18}$$

Case 2: $t \in [t_i, t_i + \Delta t]$. The corresponding motion mode of the evader is m_i, thus the state equation becomes

$$\dot{\mathbf{x}}(t) = \mathbf{A}\mathbf{x}(t) + \mathbf{B}_1 u_p(t) + \mathbf{B}_2 m_i + \mathbf{w}(t) \tag{19}$$

By virtue of Eq. (11), the form of the observer is identical with Eq. (14), because the pursuer still thinks that the evader is in the the mode m_{i-1} . It suggests that a mode mismatch occurs in this case. The state estimation error satisfies

$$\begin{aligned} \dot{\tilde{\mathbf{x}}}(t) &= (\mathbf{A} - \mathbf{k}(t)\mathbf{H})\tilde{\mathbf{x}}(t) + (\mathbf{k}(t)\mathbf{v}(t) - \mathbf{w}(t)) \\ &\quad - \mathbf{B}_2(m_i - m_{i-1}) \\ \tilde{\mathbf{x}}(t_i) &= \tilde{\mathbf{x}}_{t_i} \end{aligned} \tag{20}$$

Therefore, it is obtained that

$$\begin{aligned} \tilde{\mathbf{x}}(t) = \exp\left\{\int_{t_i}^{t} \mathbf{F}(s)\mathrm{d}s\right\} \tilde{\mathbf{x}}_{t_i} + \int_{t_i}^{t} \exp\left\{\int_{s}^{t} \mathbf{F}(u)\mathrm{d}u\right\} \xi(\mathrm{s})\mathrm{d}s \\ -(m_i - m_{i-1}) \int_{t_i}^{t} \exp\left\{\int_{s}^{t} \mathbf{F}(u)\mathrm{d}u\right\} \mathrm{d}s \cdot \mathbf{B}_2 \end{aligned} \tag{21}$$

Substituting Eq. (18) with $t = t_i$, we acquire

$$\begin{aligned} \tilde{\mathbf{x}}(t_i) = \exp\left\{\int_{t_{i-1}+\Delta t}^{t_i} \mathbf{F}(s)\mathrm{d}s\right\} \tilde{\mathbf{x}}_{t_{i-1}+\Delta t} \\ + \int_{t_{i-1}+\Delta t}^{t_i} \exp\left\{\int_{s}^{t_i} \mathbf{F}(u)\mathrm{d}u\right\} \xi(\mathrm{s})\mathrm{d}s \end{aligned} \tag{22}$$

According to Eqs. (21) and (22), it is readily got

$$\begin{aligned} \tilde{\mathbf{x}}(t) = \exp\left\{\int_{t_{i-1}+\Delta t}^{t} \mathbf{F}(s)\mathrm{d}s\right\} \tilde{\mathbf{x}}_{t_{i-1}+\Delta t} \\ + \int_{t_{i-1}+\Delta t}^{t} \exp\left\{\int_{s}^{t} \mathbf{F}(u)\mathrm{d}u\right\} \xi(\mathrm{s})\mathrm{d}s \\ - (m_i - m_{i-1}) \int_{t_i}^{t} \exp\left\{\int_{s}^{t} \mathbf{F}(u)\mathrm{d}u\right\} \mathrm{d}s \cdot \mathbf{B}_2 \end{aligned} \tag{23}$$

Notice that $E\{\mathbf{v}(t)\} = \mathbf{0}$ and $E\{\mathbf{w}(t)\} = \mathbf{0}$, which leads to

$$E\{\xi(t)\} = \mathbf{k}(t)E\{\mathbf{v}(t)\} - E\{\mathbf{w}(t)\} = \mathbf{0} \tag{24}$$

where $E\{\cdot\}$ is the mathematical expectation. Therefore, the mean error of state (denoted by $\zeta(t)$) satisfies

$$\zeta(t) = E\{\tilde{\mathbf{x}}(t)\} = \exp\left\{\int_{t_{i-1}+\Delta t}^{t} \mathbf{F}(s)\mathrm{d}s\right\} E\{\tilde{\mathbf{x}}_{t_{i-1}+\Delta t}\} - (m_i - m_{i-1})\int_{t_i}^{t} \exp\left\{\int_{s}^{t} \mathbf{F}(u)\mathrm{d}u\right\}\mathrm{d}s \cdot \mathbf{B}_2 \tag{25}$$

From Eq. (25), it is observed that $\zeta(t)$ consists of two parts. The first term on the right side measures the influence of the initial estimation error, and the second term measures the influence of the mode mismatch.

IV. MAMDD AND LRMST

Based on the above error model, in this section, MAMDD is solved given the error bound. Meanwhile, to guarantee the observabilities of mode switches, LRMST is calculated when the system mode decision delay is known.

Assume that a long time has already been worked for the filter before the maneuver of the evader, then the Kalman gain converges to a steady value. In this case, the steady-state Kalman gain $\mathbf{k}_s$ can be used to approximate $\mathbf{k}(t)$. Note that the covariance matrix of the measurement noise is range varying in terminal guidance, thus $\mathbf{k}_s$ also varies with respect to the relative range r. The expression of $\mathbf{k}_s$ is given by

$$\mathbf{k}_s = \mathbf{P}_s\mathbf{H}^{\mathrm{T}}\mathbf{R}^{-1}(r) \tag{26}$$

where $\mathbf{P}_s$ is the steady covariance matrix that obeys the following Riccati equation

$$\mathbf{0} = \mathbf{A}\mathbf{P}_s + \mathbf{P}_s\mathbf{A}^{\mathrm{T}} + \mathbf{Q} - \mathbf{P}_s\mathbf{H}^{\mathrm{T}}\mathbf{R}^{-1}(r)\mathbf{H}\mathbf{P}_s \tag{27}$$

Denote $\mathbf{F}_s = \mathbf{A} - \mathbf{k}_s\mathbf{H}$ and let $\Delta m_i = (m_i - m_{i-1})$ represent the change value of the ith mode switch. Then for $t \in [t_i, t_i + \Delta t]$, Eq. (25) can be rewritten as

$$\zeta(t) = e^{\mathbf{F}_s(t-t_{i-1}-\Delta t)}\zeta(t_{i-1} + \Delta t) - \Delta m_i \int_{t_i}^{t} e^{\mathbf{F}_s(t-s)}\mathrm{d}s \cdot \mathbf{B}_2 \tag{28}$$

After a Jordan canonical decomposition of the matrix $\mathbf{F}_s$, it is obtained that $\mathbf{F}_s = \mathbf{P}\mathbf{J}\mathbf{P}^{-1}$. Where $\mathbf{J}$ is the Jordan canonical form of $\mathbf{F}_s$, whose eigenvalues are denoted by $\lambda_i = a_i + jb_i$, $i = 1, 2, 3, 4$. From Eq. (28), it is easy to know all the real part of the eigenvalues a_i must be less than zero to ensure the convergence of filtering.

Lemma 1: Suppose that $\mathbf{A}$ is an nth-order square matrix with all different eigenvalues $\lambda_i = a_i + jb_i$, $i = 1, ..., n$. Its eigenvalues satisfy condition: $a_n < a_{n-1} < \cdots < a_1 < 0$. Then the following expression $||e^{\mathbf{A}t}|| \le \kappa(\mathbf{A})e^{a_1 t} = \kappa e^{a_1 t}$ (for brevity, $||\cdot||$ denotes the 2-norm of matrix hereafter) holds, where $\kappa = \kappa(\mathbf{A}) = ||\mathbf{P}|| \cdot ||\mathbf{P}^{-1}||$ is the condition number of $\mathbf{A}$.

The proof of Lemma 1 is given in Appendix. From Lemma 1, the following inequality can be obtained

$$||\zeta(t)|| \le \kappa e^{a_1(t-t_{i-1}-\Delta t)}||\zeta(t_{i-1} + \Delta t)|| - \frac{\Delta m_i\kappa \cdot ||\mathbf{B}_2||}{a_1} + \frac{\Delta m_i\kappa \cdot ||\mathbf{B}_2||}{a_1}e^{a_1(t-t_i)} \triangleq g(t) \tag{29}$$

Notice that $a_1 < 0$, thus $g(t)$ is monotonically decreasing for $t < t_i$. It is assumed that $||\zeta(t_{i-1}+\Delta t)||$ satisfies the following inequality at $t = t_i$

$$e^{a_1(t_i-t_{i-1}-\Delta t)}||\zeta(t_{i-1} + \Delta t)|| < -\frac{\Delta m_i \cdot ||\mathbf{B}_2||}{a_1} \tag{30}$$

then $g(t)$ is monotonically increasing for $t \in [t_i, t_i + \Delta t]$. The proof is given in Appendix. Therefore, the filtering process is divergent during $t \in [t_i, t_i + \Delta t]$. That is, the mode decision delay Δt should be limited to ensure that the estimation error does not exceed the error bound.

Let E_0 denote the error bound (i.e., $||\zeta(t)|| \le E_0$), $E \triangleq E_0/\Delta m_i$ and $E_\infty \triangleq \lim_{t,\Delta t\to\infty} g(t)/\Delta m_i = -\kappa \cdot ||\mathbf{B}_2||/a_1$ denote the normalized error bound and the normalized error limit, respectively. By definition, $E < E_\infty$. As $g(t)$ is monotonically increasing for $t \in [t_i, t_i + \Delta t]$, then substituting Eq. (29) with $t = t_i + \Delta t$ and limiting its value to the error bound E_0 yields

$$g(t_i + \Delta t) = \kappa e^{a_1(t_i-t_{i-1})}||\zeta(t_{i-1} + \Delta t)|| - \frac{\Delta m_i\kappa \cdot ||\mathbf{B}_2||}{a_1} + \frac{\Delta m_i\kappa \cdot ||\mathbf{B}_2||}{a_1}e^{a_1\Delta t} \le E_0 \tag{31}$$

and

$$-\frac{\Delta m_i \cdot \kappa||\mathbf{B}_2||}{a_1} + \frac{\Delta m_i \cdot \kappa||\mathbf{B}_2||}{a_1}e^{a_1\Delta t} \le E_0 - \kappa e^{a_1(t_i-t_{i-1})}||\zeta(t_{i-1} + \Delta t)|| \le E_0 \tag{32}$$

From Eq. (32), MAMDD is specified as follows

$$\mathrm{MAMDD} = \frac{1}{a_1}\ln\left(1 + \frac{E_0 a_1}{\Delta m_i \cdot \kappa||\mathbf{B}_2||}\right) \tag{33}$$

If $\Delta t \le$ MAMDD, to ensure that Eq. (31) is true, the mode sojourn time $s_i \triangleq t_i - t_{i-1}$ still needs to be constrained. Given the mode decision delay Δt, from Eq. (31), it is acquired that

$$e^{a_1(t_i-t_{i-1})}||\zeta(t_{i-1} + \Delta t)|| \le e^{a_1(t_i-t_{i-1})}E_0 \le \frac{E_0}{\kappa} + \frac{\Delta m_i \cdot ||\mathbf{B}_2||}{a_1}\left(1 - e^{a_1\Delta t}\right) \tag{34}$$

Then, LRMST can be calculated as follows

$$\mathrm{LRMST} = \frac{1}{a_1}\ln\left(\frac{1}{\kappa} + \frac{\Delta m_i \cdot ||\mathbf{B}_2||}{a_1 E_0}\left(1 - e^{a_1\Delta t}\right)\right) \tag{35}$$

V. SIMULATIONS

To validate the above theoretical derivation, the results are compared with the Monte Carlo simulation through a typical instance of tactical ballistic missile interception. Table 1 summarizes the interception parameters. Table 2 lists the estimator's parameters. The Monte Carlo simulation number is

TABLE 1. Interception Parameters.

Parameter	Value	Unit
V_p	2300	m/s
V_e	2700	m/s
$a_p^{\max}$	30	g
$a_e^{\max}$	15	g
τ_p	0.2	s
τ_e	0.2	s
r_0	15	km
$\phi_p(0)$	$\pi/18$	rad
$\phi_e(0)$	satisfies Collision Triangle	rad
$u_p(0)$	0	g
$a_p(0)$	0	g
$a_e(0)$	$a_e^{\max}$	g

TABLE 2. Estimator's Parameters.

Parameter	Value	Unit
s_w	1	g^2/Hz
$\hat{x}(0)$	$[0,0,0,0]^T$	-
$\tilde{x}(0)$	$[0,0,a_e^{\max},0]^T$	-
P_0	$\begin{bmatrix} 0 & 0 & 0 & 0 \\ 0 & 0 & 0 & 0 \\ 0 & 0 & (a_e^{\max})^2 & 0 \\ 0 & 0 & 0 & 0 \end{bmatrix}$	-

1000 and the gravity acceleration g = 9.8 m/s^2. The measurement accuracies of the angular and the pursuer's acceleration of the radar are set to be 5 mrad and 1 m/s^2, respectively. A maneuver of the evader occurs at $t = 2.0$s and the mode decision delay is set to be 0.1 s. A bang-bang control strategy is adopted by the evader as it can minimize the capture zone of the pursuer [18]. Without loss of generality, only a single mode change is considered here.

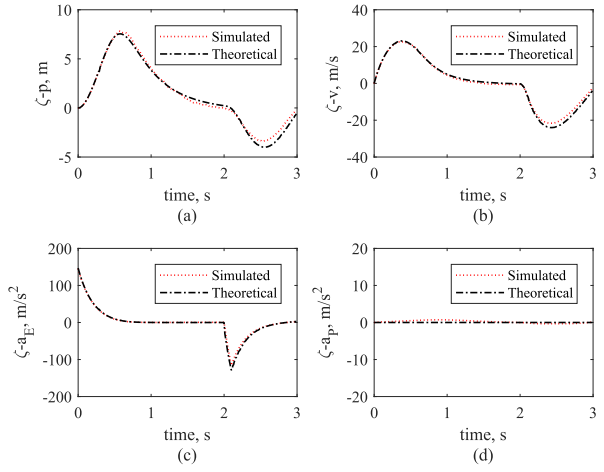

FIGURE 5. Estimation error of every state with respect to time. (a) error of relative position; (b) error of relative velocity; (c) error of evader's lateral acceleration; (d) error of pursuer's acceleration. The mode switch occurs at $t = 2.0$s and the mode decision delay $\Delta t = 0.1$s.

Fig. 5 shows the estimation error of every state with respect to time. It is seen from this figure that the curves of Monte Carlo simulation match well with the analytic results, which proves the correctness of the derived error model. Furthermore, it can be observed that after the former 2 second filtering, the initial state estimation errors $\tilde{\mathbf{x}}_0$ gradually converges to zero; when the evader's mode changes ($t = 2$s), mode mismatch occurs and the estimation errors of the relative position, the relative velocity and the evader's lateral acceleration increase quickly; after the mode is correctly identified ($t = 2.1$s), the state estimation error then converges asymptotically. However, the estimation of the pursuer's acceleration is not affected by the mode mismatch and its error remains a very small value during the whole interception. This is in accordance with the assumption that an accurate acceleration model of the pursuer is available and its value can be measured by the seeker onboard precisely.

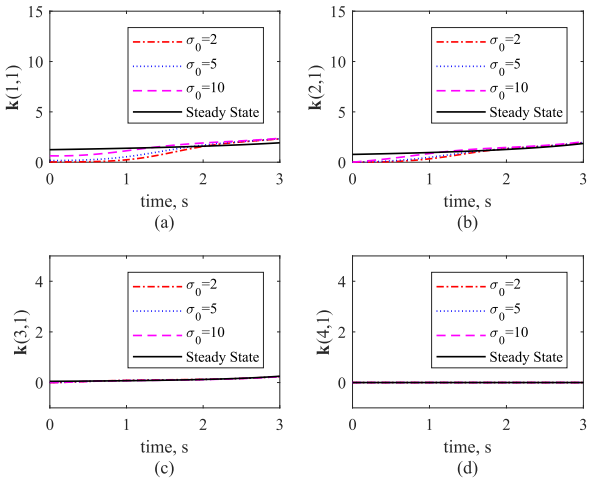

FIGURE 6. Kalman gains with respect to time under different initial conditions. (a) gain of relative position; (b) gain of relative velocity; (c) gain of evader's lateral acceleration; (d) gain of pursuer's acceleration.

Fig. 6 illustrates the results of the current Kalman gain and the steady gain with respect to time under different initial conditions ($\mathbf{P}_0 = \sigma_0^2\mathbf{I}_4$). As the relative range r decreases with the time-to-go, $\mathbf{R}$ decreases with the decrease of r. By virtual of Eq. (26), $\mathbf{k}(t)$ and $\mathbf{k}_s$ increase with time. As shown in Fig. 6, after a certain period of iteration, $\mathbf{k}(t)$ gradually approaches $\mathbf{k}_s$. Therefore, it is proper to replace $\mathbf{k}(t)$ with $\mathbf{k}_s$ when calculating MAMDD and LRMST.

Fig. 7 shows the results of MAMDD and LRMST. Specifically, a) presents the relationship between E_∞ and r. E_∞ measures the limit of normalized error bound for different relative range. It is seen from this figure that E_∞ increases with the increase of r. That is, the farther the relative range, the greater the allowable error. As r increases, the variance of the measurement noise increases and $\mathbf{k}_s$ decreases (see Eq. (26)). Then, the real part a_1 of the maximum eigenvalue of $\mathbf{F}_s$ increases, which further leads to the increase of E_∞. b) shows the relationship between MAMDD and the normalized error bound E for different r. It is observed that MAMDD increases with the increase of E, thus the requirement of the mode decision-maker get more relaxed for a larger E. Given MAMDD, a smaller relative range r means a lower error bound E. That is, a more stringent requirement should be applied to the mode decision-maker as the players

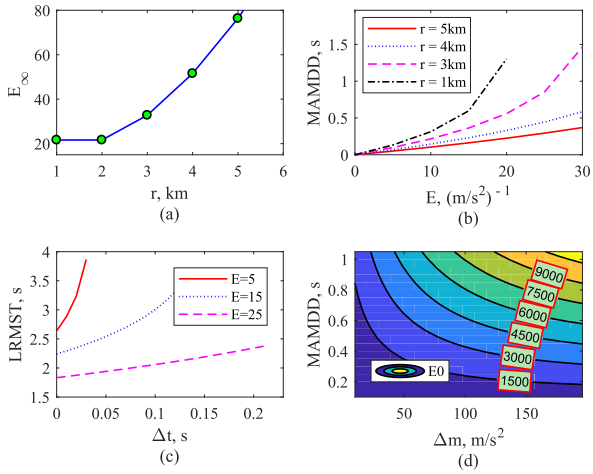

FIGURE 7. MAMDD and LRMST. (a) E_∞ with respect to range; (b) MAMDD with respect to for different range; (c) LRMST with respect to Δt for different E; (d) E_0 under different Δm and MAMDD.

get closer. c) shows the relationship between LRMST and Δt for $r = 5$ km. As shown in this figure, given the error bound, LRMST increases with the mode decision delay, which is in accordance with Eq. (34). When the mode decision delay is settled, the smaller the error bound E, the greater the LRMST. In other words, as the admissible error bound becomes lower, the mode sojourn time needs to be longer to ensure that the mode switches are observable and the estimation error does not exceed the bound. d) gives the contour map of E_0 as a function of MAMDD and Δm for $r = 5$ km. It can be found from this figure that MAMDD is approximately inversely proportional to Δm. That is, a stricter requirement is applied to the mode decision-maker when intercepting a target with a higher maneuverability.

TABLE 3. Comparison of MAMDD(s) with respect to E for r = 5km.

E (s^2/m)	15	30	45	60	75
Results of [17]	0.1633	0.3732	0.6672	1.1619	3.3866
Proposed method	0.1620	0.3696	0.6592	1.1414	2.9916

Table 3 compares the values of MAMDD given in [17] and this paper for different normalized error bounds when $r = 5$km. It is observed that the results of this paper are smaller than its results in [17] especially for a larger E. That is, a more precise requirement for the mode decision-maker is presented in this paper.

In practice, one can use the derived MAMDD and LRMST to make requirements for the mode decision-maker in IEG system design and evaluate the performance of the estimator in hybrid system.

VI. CONCLUSION

As a counterpart of [17], two critical parameters MAMDD and LRMST of the logic-based IEG system in continuous-time controlled system are derived. Simulation results show that MAMDD increases with the increase of error bound. As the pursuer approaches the evader, the requirement of identifying the evader's mode for the mode decision-maker gets more stringent. Given an error bound, the smaller the mode decision delay, the longer the mode sojourn time is required to ensure the observability of mode switches. A more relaxed requirement is applied to the mode decision-maker when intercepting the evader with a weaker maneuverability. The bounds derived in this paper are more compact than its discrete counterpart. Conclusions in this paper give a useful tool for guiding the design of the mode decision-maker in a practical IEG control system, especially for the determination of mode decision delay.

To reduce the decision delay of target maneuver, the design of feature-aided mode decision-maker is our future work.

APPENDIXES

Proof of Lemma 1: Assume that $\mathbf{A} = \mathbf{P}\mathbf{J}\mathbf{P}^{-1}$ and its distinct eigenvalues $\lambda_i = a_i + jb_i$, $i = 1, ..., n$ satisfy $a_n < a_{n-1} < \cdots < a_1 < 0$, then

$$\begin{aligned} \mathrm{e}^{\mathbf{A}t} &= \mathbf{P}\begin{pmatrix} \mathrm{e}^{a_1 t + jb_1 t} & & \\ & \ddots & \\ & & \mathrm{e}^{a_n t + jb_n t} \end{pmatrix}\mathbf{P}^{-1} \\ &= \mathbf{P}f(\mathbf{J}_t)\mathbf{P}^{-1} \end{aligned} \tag{36}$$

According to the characteristic of norm-2, following inequality can be obtained

$$||\mathrm{e}^{\mathbf{A}t}|| = ||\mathbf{P}f(\mathbf{J}_t)\mathbf{P}^{-1}|| \le ||\mathbf{P}|| \cdot ||\mathbf{P}^{-1}|| \cdot ||f(\mathbf{J}_t)|| \tag{37}$$

and

$$\begin{aligned} ||f(\mathbf{J}_t)|| &= \rho^{1/2}\left(f^{\mathrm{H}}(\mathbf{J}_t)\cdot f(\mathbf{J}_t)\right) \\ &= \rho^{1/2}\left(\begin{pmatrix} e^{2a_1 t} & & \\ & \ddots & \\ & & e^{2a_n t} \end{pmatrix}\right) = e^{a_1 t} \end{aligned} \tag{38}$$

where $\rho(\cdot)$ is the function of spectral radius. Then

$$||e^{\mathbf{A}t}|| \le \kappa(\mathbf{A})e^{a_1 t} = \kappa e^{a_1 t} \tag{39}$$

this completes the proof of Lemma 1.

Proof the monotonicity of $g(t)$: For $t \in [t_i, t_i + \Delta t]$, differentiate the $g(t)$ with respect to the time t, it can be obtained

$$\begin{aligned} g'(t) &= \kappa a_1 e^{a_1(t-t_{i-1}-\Delta t)}||\zeta(t_{i-1}+\Delta t)|| \\ &\quad + \Delta m_i \kappa \cdot ||\mathbf{B}_2|| e^{a_1(t-t_i)} \\ &= \kappa a_1 e^{a_1(t-t_i+t_i-t_{i-1}-\Delta t)}||\zeta(t_{i-1}+\Delta t)|| \\ &\quad + \Delta m_i \kappa \cdot ||\mathbf{B}_2|| e^{a_1(t-t_i)} \\ &= \kappa e^{a_1(t-t_i)} \cdot a_1 e^{a_1(t_i-t_{i-1}-\Delta t)}||\zeta(t_{i-1}+\Delta t)|| \\ &\quad + \kappa e^{a_1(t-t_i)}\Delta m_i \cdot ||\mathbf{B}_2|| \end{aligned} \tag{40}$$

then from (30), we can acquire $g'(t) > 0$. Therefore, $g(t)$ is monotone increasing in this time interval. This completes the proof.

Proof of Eq. (30): To meet the system requirements, following conditions should be guaranteed: $||\zeta(t_{i-1} + \Delta t)|| \leq E_0$, $t_i - t_{i-1} \geq$ LRMST and $\Delta t \leq$ MAMDD. Therefore,

$$\begin{aligned}
&e^{a_1(t_i - t_{i-1} - \Delta t)}||\zeta(t_{i-1} + \Delta t)|| \\
&\leq e^{a_1 \cdot \text{LRMST}} e^{-a_1 \cdot \text{MAMDD}} E_0 \\
&= \left(\frac{1}{\kappa} + \frac{\Delta m_i \cdot ||\mathbf{B}_2||}{a_1 E_0}\left(1 - e^{a_1 \Delta t}\right)\right) e^{-a_1 \cdot \text{MAMDD}} E_0 \\
&\leq \left(\frac{1}{\kappa} + \frac{\Delta m_i \cdot ||\mathbf{B}_2||}{a_1 E_0}\left(1 - e^{a_1 \cdot \text{MAMDD}}\right)\right) e^{-a_1 \cdot \text{MAMDD}} E_0 \\
&= \left(\frac{E_0}{\kappa} + \frac{\Delta m_i \cdot ||\mathbf{B}_2||}{a_1}\right) e^{-a_1 \cdot \text{MAMDD}} - \frac{\Delta m_i \cdot ||\mathbf{B}_2||}{a_1} \\
&= \left(\frac{E}{\kappa} - \frac{E_\infty}{\kappa}\right) \cdot \Delta m_i e^{-a_1 \cdot \text{MAMDD}} - \frac{\Delta m_i \cdot ||\mathbf{B}_2||}{a_1} \\
&< -\frac{\Delta m_i \cdot ||\mathbf{B}_2||}{a_1}
\end{aligned} \tag{41}$$

this completes the proof of Eq. (30).

REFERENCES

[1] M. E. Hough, "Reentry maneuver estimation using nonlinear Markov acceleration models," *J. Guid., Control, Dyn.*, vol. 40, no. 7, pp. 1693–1710, 2017.
[2] G. S. Kumar, R. Ghosh, D. Ghose, and A. Vengadarajan, "Guidance of seekerless interceptors using innovation covariance based tuning of Kalman filters," *J. Guid., Control, Dyn.*, vol. 40, no. 3, pp. 603–614, 2017.
[3] S. M. He, W. Wang, and J. Wang, "Three-dimensional multivariable integrated guidance and control design for maneuvering targets interception," *J. Franklin Inst.*, vol. 353, no. 16, pp. 4330–4350, 2016.
[4] A. B. Bryson and Y.-C. Ho, *Applied Optimal Control*. Philadelphia, PA, USA: Hemisphere, 1975, pp. 422–428.
[5] X. R. Li and V. P. Jilkov, "Survey of maneuvering target tracking: Decision-based methods," *Proc. SPIE*, vol. 4728, pp. 511–535, Aug. 2002.
[6] X. R. Li and V. P. Jilkov, "Survey of maneuvering target tracking. Part V. Multiple-model methods," *IEEE Trans. Aerosp. Electron. Syst.*, vol. 41, no. 4, pp. 1255–1321, Oct. 2005.
[7] J. Ru, A. Bashi, and X.-R. Li, "Performance comparison of target maneuver onset detection algorithms," *Proc. SPIE*, vol. 5428, pp. 419–429, Aug. 2004.
[8] J. Shinar, V. Turetsky, and V. Y. Glizer, "On estimation in interception endgames," *J. Optim. Theory Appl.*, vol. 157, no. 3, pp. 593–611, 2013.
[9] J. Shinar and T. Shima, "Nonorthodox guidance law development approach for intercepting maneuvering targets," *J. Guid., Control, Dyn.*, vol. 25, no. 4, pp. 658–666, 2002.
[10] V. Y. Glizer and V. Turetsky, "A linear differential game with bounded controls and two information delays," *Optim. Control Appl. Methods*, vol. 30, no. 2, pp. 135–161, 2009.
[11] H. Q. Fan, "Technology on maneuvering target motion mode identification in active homing guidance," Ph.D. dissertation, Nat. Key Lab. Sci. Technol. ATR, National Univ. Defense Technol., Changsha, China, 2008.
[12] Y. Zhu, H. Fan, J. Fan, Z. Lu, and Q. Fu, "Target turning maneuver detection using high resolution Doppler profile," *IEEE Trans. Aerosp. Electron. Syst.*, vol. 48, no. 1, pp. 762–779, Jan. 2012.
[13] S.-J. Fan, H.-T. Xiao, H.-Q. Fan, and J.-P. Fan, "Target maneuver discrimination using ISAR image in interception," *EURASIP J. Adv. Signal Process.*, vol. 2016, p. 24, Feb. 2016.
[14] D. Dionne, H. Michalska, J. Shinar, and Y. Oshman, "Decision-directed adaptive estimation and guidance for an interception endgame," *J. Guid., Control Dyn*, vol. 29, no. 4, pp. 970–980, 2006.
[15] J. Shinar, V. Turetsky, and Y. Oshman, "Integrated estimation/guidance design approach for improved homing against randomly maneuvering targets," *J. Guid., Control, Dyn.*, vol. 30, no. 1, pp. 154–161, 2007.
[16] S. K. Gour, D. Ghose, and A. Vengadarajan, "A novel IEG strategy for realistically modeled seeker-less interceptors," in *Proc. AIAA Guid., Navigat., Control Conf.*, Kissimmee, FL, USA, 2013, pp. 1–19.
[17] H. Fan, Y. Zhu, and Q. Fu, "Impact of mode decision delay on estimation error for maneuvering target interception," *IEEE Trans. Aerosp. Electron. Syst.*, vol. 47, no. 1, pp. 702–711, Jan. 2011.
[18] V. Turetsky and J. Shinar, "Missile guidance laws based on pursuit–evasion game formulations," *Automatica*, vol. 39, no. 4, pp. 607–618, 2003.
[19] X. R. Li, Z. Zhao, and X.-B. Li, "General model-set design methods for multiple-model approach," *IEEE Trans. Autom. Control*, vol. 50, no. 9, pp. 1260–1276, Sep. 2005.
[20] Y. Liang, X. R. Li, C. Han, and Z. Duan, "A general systematic method for model-set design," *IEEE Trans. Aerosp. Electron. Syst.*, vol. 39, no. 2, pp. 1505–1520, Apr. 2012.
[21] L. A. Petrosjan, *Differential Games of Pursuit* (Series on Optimization), vol. 2. Singapore: World Scientific, 1993.

SHENGWEN XIANG was born in Huaihua, Hunan, China, in 1991. He received the B.S. degree in communication engineering from Hunan University, Changsha, China, in 2013, and the M.S. degree in information and communication engineering from the National University of Defense Technology, Changsha, in 2015, where he is currently pursuing the Ph.D. degree.

His main research interests image processing, target tracking, guidance, and control.

HONGQI FAN was born in Weinan, Shaanxi, China, in 1978. He received the B.S. degree in mechanical engineering from Tsinghua University, Beijing, China, in 2001, and the M.S. and Ph.D. degrees in information and communication engineering from the National University of Defense Technology (NUDT), Changsha, China, in 2003 and 2005, respectively.

He is currently an Associate Professor with the National Key Laboratory of Science and Technology on ATR, NUDT. His research interests include radar signal processing, target tracking, guidance and control, and information fusion.

QIANG FU received the B.S. and the Ph.D. degrees in information and communication engineering from the National University of Defense Technology (NUDT), Changsha, China, in 1983 and 2004, respectively.

He is currently a Professor with the National Key Laboratory of Science and Technology on ATR, NUDT. His main research interest includes the radar system design, precise guidance, and automatic target recognition.